Interaction of Cationic Porphyrins with DNA: Importance of the Number and Position of the Charges and Minimum Structural Requirements for Intercalation

M. A. Sari,[‡] J. P. Battioni,[‡] D. Dupré,[‡] D. Mansuy,*[,‡] and J. B. Le Pecq[§]

Laboratoire de Chimie et Biochimie Pharmacologiques et Toxicologiques (UA 400 CNRS), Université René Descartes, 45 rue des Saints-Pères, 75270 Paris Cedex 06, France, and Laboratoire de Physico-Chimie Macromoléculaire (LA 147 CNRS, U140 INSERM), Institut Gustave Roussy, 94800 Villejuif, France

Received August 2, 1989; Revised Manuscript Received December 11, 1989

ABSTRACT: Thirty-three porphyrins or metalloporphyrins corresponding to the general formula [*meso*-[*N*-methyl-4(or 3 or 2)-pyridiniumyl]$_n$(aryl)$_{4-n}$porphyrin]M (M = H_2, Cu^{II}, or $ClFe^{III}$), with n = 2–4, have been synthesized and characterized by UV–visible and ^{1}H NMR spectroscopy and mass spectrometry. These porphyrins differ not only in the number (2–4) and position of their cationic charges but also in the steric requirements to reach even temporarily a completely planar geometry. In particular, they contain 0, 1, 2, 3, or 4 *meso*-aryl substituents not able to rotate. Interaction of these porphyrins or metalloporphyrins with calf thymus DNA has been studied and their apparent affinity binding constants have been determined by use of a competition method with ethidium bromide which was applicable not only for all the free base porphyrins but also for their copper(II) or iron(III) complexes. Whatever their mode of binding may be, their apparent affinity binding constants were relatively high (K_{app} between 1.2×10^7 and 5×10^4 M^{-1} under our conditions), and a linear decrease of log K_{app} with the number of porphyrin charges was observed. Studies of porphyrin–DNA interactions by UV and fluorescence spectroscopy, viscosimetry, and fluorescence energy transfer experiments showed that not only the tetracationic *meso*-tetrakis[*N*-methyl-4(or 3)-pyridiniumyl]porphyrins, which both involved four freely rotating *meso*-aryl groups, but also the corresponding tri- and dicationic porphyrins were able to intercalate into calf thymus DNA. Moreover, the cis dicationic *meso*-bis(*N*-methyl-2-pyridiniumyl)diphenylporphyrin, which involved only two freely rotating *meso*-aryl groups in a cis position, was also able to intercalate. The other *meso*-(*N*-methyl-2-pyridiniumyl)$_n$(phenyl)$_{4-n}$porphyrins, which involved either zero, one, or two trans freely rotating *meso*-aryl groups, could not intercalate into DNA. These results show that *only half of the porphyrin ring is necessary for intercalation to occur.*

Since the first report of Fiel and co-workers (Fiel et al., 1979), a number of studies have confirmed that the cationic *meso*-tetrakis(*N*-methyl-4-pyridiniumyl)porphyrin[1] (Figure 1) is able to bind to DNA, with a high affinity: 10^7–10^6 M^{-1} (Fiel et al., 1979; Pasternack et al., 1983a; Kelly et al., 1985; Dougherty et al., 1985). Metal complexes of this porphyrin with no axial ligands or weak axial ligands [such as Cu(II), Ni(II), and Au(III) complexes] as well as its isomer tetrakis(*N*-methyl-3-pyridiniumyl)porphyrin also behave as intercalating drugs. This was shown by using various techniques,[2] such as UV and fluorescence spectroscopy, viscosimetry, unwinding of supercoiled DNA, and circular or linear dichroism, as well as ^{1}H and ^{31}P NMR, ESR and Raman spectroscopy, and kinetic methods (Banville et al., 1983, 1986; Blom et al., 1986; Carvlin et al., 1982, 1983; Carvlin & Fiel, 1983; Dougherty et al., 1985; Fiel et al., 1979, 1980, 1985; Geacintov et al., 1987; Gibbs et al., 1988a,b; Kelly et al., 1985; Marzilli et al., 1986; Pasternack et al., 1983a,b, 1984, 1985, 1986; Sari et al., 1986, 1988; Strickland et al., 1987, 1988, 1989).

Moreover, studies performed on synthetic oligonucleotides provided further insight into the specificity of this binding (Banville et al., 1983, 1986; Carvlin & Fiel, 1983; Fiel et al., 1985; Kelly et al., 1985; Marzilli et al., 1986; Pasternack et al., 1983a,b, 1984; Strickland et al., 1987). Taken together with measurements performed at various ionic strengths (Carvlin & Fiel, 1983; Dougherty et al., 1985; Fiel et al., 1985; Pasternack et al., 1986), these results indicate that these tetracationic porphyrins are able to intercalate into DNA, especially at the level of GC-containing sequences and presumably at 5′-CG sites (Banville et al., 1983), at low [porphyrin]:[DNA] ratio and at low ionic strength. When the [porphyrin]:[DNA] ratio and/or ionic strength increases, the mode of binding becomes more complex and involves both intercalation at GC sites and outside binding which occurs predominantly at AT sites (Ford et al., 1987a; Ward et al., 1986).

On the contrary, metal complexes of tetrakis(*N*-methyl-4-pyridiniumyl)porphyrin containing strong axial ligands and tetrakis(*N*-methyl-2-pyridiniumyl)porphyrin, which cannot exist even transiently in a completely planar conformation either because of the presence of the strong axial ligand or because of the lack of rotation of the four *meso*-aryl groups, only bind externally to DNA, more specifically in AT regions (Banville et al., 1983, 1986; Fiel et al., 1985; Kelly et al., 1985; Pasternack et al., 1983a, 1984; Strickland et al., 1987; Ward et al., 1986).

To date, only tetracationic (*N*-methylpyridiniumyl)-porphyrins have been extensively studied, and apparent binding constants for DNA have been determined only for tetrakis-(*N*-methyl-4(or 3)-pyridiniumyl]porphyrins by UV spectroscopy (Fiel et al., 1979; Pasternack et al., 1983a,b; Dougherty

[‡] Université René Descartes.
[§] Institut Gustave Roussy.

[1] Abbreviations: EB, ethidium bromide; CT DNA, calf thymus DNA; K_{app}, apparent affinity binding constant of a porphyrin for CT DNA. For porphyrins, see Figure 1.

[2] For a review about the physicochemical evidences of intercalation, see Dougherty and Pilbrow (1985).

0006-2960/90/0429-4205$02.50/0

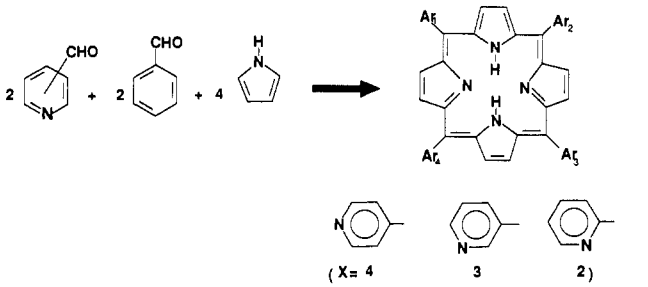

	(X= 4	3	2)
$Ar_1 = Ar_2 = Ar_3 = Ar_4 = X$ - N - pyridyl	P4	M4	O4
$Ar_1 = Ph$; $Ar_2 = Ar_3 = Ar_4 = X$ - N - pyridyl	P3	M3	O3
$Ar_1 = Ar_2 = Ph$; $Ar_3 = Ar_4 = X$ - N - pyridyl	P2-cis	M2-cis	O2-cis
$Ar_1 = Ar_3 = Ph$; $Ar_2 = Ar_4 = X$ - N - pyridyl	P2-trans	M2-trans	O2-trans
$Ar_1 = Ar_2 = Ar_3 = Ph$; $Ar_4 = X$ - N - pyridyl	P1	M1	O1

FIGURE 1: Synthesis and abbreviations of *meso*-[*N*-methyl-4(or 3 or 2)-pyridyl]$_n$(phenyl)$_{4-n}$porphyrins.

et al., 1985; Kelly et al., 1985), the equilibrium dialysis technique having been used so far only for measurements of binding constants for polynucleotides (Strickland et al., 1988, 1989). There are only few reports on the interaction of DNA with less charged porphyrins. Our preliminary results concerning only the (*N*-methyl-4-pyridiniumyl)$_n$(phenyl)$_{4-n}$porphyrin series containing between 2 and 4 charges showed that these porphyrins were also able to intercalate into DNA and exhibited relatively high global apparent binding constants for CT DNA (Sari et al., 1986). Dabrowiack and co-workers (Bromley et al., 1986) have confirmed, by footprinting experiments performed with nonintercalating manganese complexes of various (*N*-methylpyridiniumyl)$_{4-n}$(tolyl)$_n$porphyrins, that changes in position and total number of cationic charges have little influence on the DNA binding specificity. Very recently, the interaction of dicationic *cis*- and *trans-meso*-bis(*N*-methyl-4-pyridiniumyl)diphenylporphyrins with oligonucleotides and CT DNA was studied by UV and circular dichroism spectroscopy (Gibbs et al., 1988b). These results supported a model of intercalation of these two porphyrins only at low ionic strength but were in favor of their external binding to form long-range stacked structures on the exterior of nucleic acids because of their tendency to aggregate at high ionic strength.[3]

To evaluate the influence of the number and spatial orientation of the positive charges, as well as the influence of the steric hindrance of meso substituents or of the coordination of metals on the interactions of cationic porphyrins with DNA, we have prepared the complete series of *meso*-[*N*-methyl-4(or 3 or 2)-pyridiniumyl]$_n$(phenyl)$_{4-n}$porphyrins (n = 2–4) and their copper(II) and chloroiron(III) complexes. In particular, we have prepared cationic porphyrins involving only 1, 2 (cis or trans), 3, or 4 *meso*-aryl groups that cannot rotate in order to determine the smallest planar area that a porphyrin must present to be able to intercalate into DNA.

In this article, we report a brief description of their synthesis and spectral characteristics and a detailed investigation of their binding to CT DNA.[4] UV–visible spectroscopy, viscosimetry, and fluorescence energy transfer experiments have been performed to study the mode of interaction of these porphyrins with CT DNA. Moreover, all the apparent binding constants have been determined by using competition experiments with ethidium bromide which allow such a determination even for outside-binding porphyrins.

[3] During the preparation of the manuscript, a review article on porphyrin–nucleic acid interactions appeared (Fiel, 1989).

[4] A preliminary communication of these results has been presented at the International Congress on Nucleic Acid Interactions, Padova, Italy, 1987 (Sari et al., 1988).

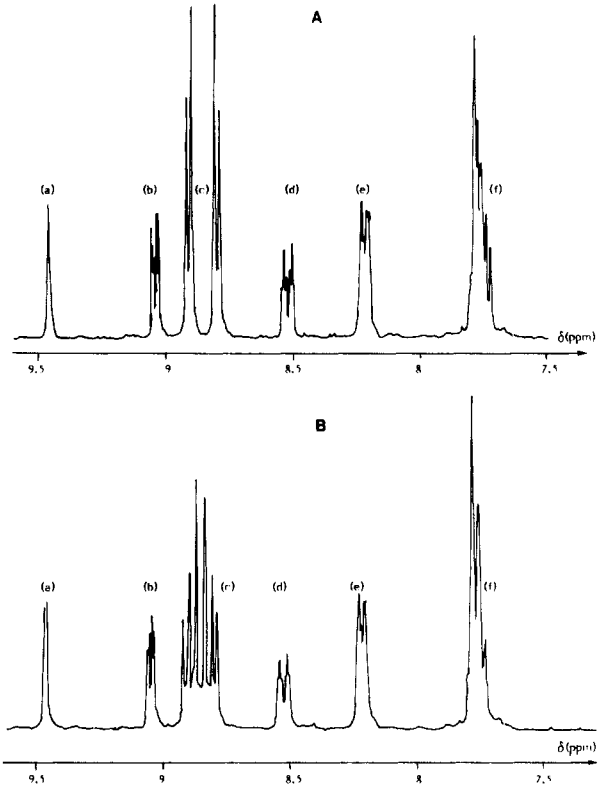

FIGURE 2: ^{1}H NMR of *cis*- and *trans-meso*-di-3-pyridyldiphenylporphyrins. 7.4–9.6 ppm region of the ^{1}H NMR spectra of the porphyrins M2-trans (A) and M2-cis (B) in $CDCl_3$ [δ in ppm relative to $(CH_3)_4Si$]. Signal assignments: (a) 2-Py (2 H), (b) 4-Py (2 H), (d) 6-Py (2 H), (e) *o*-Ph (4 H), and (f) *m*- and *p*-Ph and 5-Py (8 H). Signal c allows us to assign the porphyrin configuration: two doublets (4 H × 2) in (A) indicative of the D_{2h} symmetry corresponding to the trans isomer, and two singlets (2 H × 2) and two doublets (2 H × 2) in (B) indicative of the C_{2v} symmetry of the cis isomer.

Materials and Methods

Reagents (analytical grade) were used without further purification. Calf thymus DNA was purchased from Boehringer and sonicated as previously described (Le Pecq & Paoletti, 1967).

Porphyrin Synthesis. Porphyrins corresponding to the general formula *meso*-(*X*-pyridyl)$_n$(phenyl)$_{4-n}PH_2$, with X = 4- (para), 3- (meta), or 2- (ortho) (see Figure 1), were prepared from pyrrole, benzaldehyde, and, respectively, 4-, 3-, or 2-pyridinecarboxaldehyde according to the mixed-aldehyde method described by Little et al. (1975). For each pyridinecarboxaldehyde, these reactions led to a mixture of six porphyrins which were separated on preparative Florisil chromatography columns, eluted with CH_2Cl_2 and increasing amounts of a more polar solvent. The percentage of acetone or methanol used to elute the various porphyrins is indicated below. For the three series (P, M, or O), the order of elution was tetraphenyl-, monopyridyl-, *trans*-dipyridyl-, *cis*-dipyridyl-, tripyridyl-, and tetrapyridyl- meso-substituted porphyrin.

All these porphyrins were characterized by mass spectrometry and UV–visible and ^{1}H NMR spectroscopy. In the following, for each porphyrin, we have indicated (in order) the proportion of polar solvent used in addition to CH_2Cl_2 to elute it, the major peak(s) of its mass spectrum (NH_3 chemical ionization), its UV–visible data (in CH_2Cl_2, λ in nm, ϵ in $mM^{-1}\cdot cm^{-1}$), and its ^{1}H NMR signals corresponding to the pyrrole protons (J in Hz). The pyrrole signals were always mentioned as they are indicative of the porphyrin structure. In particular, they allowed us to easily distinguish between

the two cis and trans P2, M2, or O2 isomers because of the different symmetry of the porphyrin ring (C_{2v} and D_{2h} for the cis and trans isomers, respectively). This is illustrated in Figure 2 which compares the ^{1}H NMR spectra of M2-cis and M2-trans. The other signals of the ^{1}H NMR spectra which correspond to the *meso*-aryl groups were found to be almost independent of the number and position of the pyridyl rings within a given series (P, M, or O). They are as follows [in $DCCl_3$, δ in ppm from $(CH_3)_4Si$, J in Hz]: (P series) 3,5-Py 9.1–9.4 (d, J = 6 Hz), 2,6-Py 8.2 (m), *o*-Ph 8.2 (m), *m*- and *p*-Ph 7.8–7.7 (m), NH −2.8 (2 H, s); (M series) 2-Py 9.45 (d, J = 1.5 Hz), 4-Py 9.05 (dd, J = 5 Hz, J = 1.5 Hz), 5-Py 7.7 (m), 6-Py 8.5 (m), *o*-Ph 8.25 (m), *m*- and *p*-Ph 7.9–7.8 (m), NH −2.8 (2 H, s); (O series) 3-Py 9.1 (dd, J = 5 Hz, J = 1.5 Hz), 6-Py 8.2 (m), 5-Py 8.1 (dt, J = 5 Hz, J = 1.5 Hz), 4-Py 7.75 (m), *o*-Ph 8.2 (m), *m*- and *p*-Ph 7.9–7.7 (m), NH −2.85 (2 H, s).

meso-Tetra-4-pyridylporphyrin (*P4*): 10% methanol; m/e = 618 (M^+, 100%); UV–vis, 418 (400), 514 (18), 549 (6), 590 (5), 647 (3); NMR, pyrr 8.80 (8 H, s). *meso-Tri-4-pyridylphenylporphyrin* (*P3*): 2% methanol; m/e = 617 (M^+, 100%); UV–vis, 414 (410), 510 (19), 544 (6), 588 (5), 642 (3); NMR, pyrr 8.92 (2 H, d, J = 7), 8.85 (4 H, s), 8.81 (2 H, d, J = 7). *cis-meso-Di-4-pyridyldiphenylporphyrin* (*P2-cis*): 20–50% acetone; m/e = 617 (M^+ + 1, 100%); UV–vis, 414 (410), 512 (17), 544 (7), 586 (6), 642 (3); NMR, pyrr 8.90 (2 H, d, J = 5), 8.87 (2 H, s), 8.83 (2 H, s), 8.78 (2 H, d, J = 5). *trans-meso-Di-4-pyridyldiphenylporphyrin* (*P2-trans*): 5–15% acetone; m/e = 616 (M^+, 100%); UV–vis, 418 (420), 510 (17), 544 (6), 586 (6), 642 (3); NMR, pyrr 8.90 (4 H, d, J = 5), 8.80 (4 H, d, J = 5). *meso-4-Pyridyltriphenylporphyrin* (*P1*): 1–5% acetone; m/e = 615 (M^+, 100%); UV–vis, 417 (440), 512 (18), 544 (7), 586 (5), 642 (3); NMR, pyrr 8.89 (2 H, d, J = 7), 8.86 (4 H, s), 8.78 (2 H, d, J = 7).

meso-Tetra-3-pyridylporphyrin (*M4*): 5% methanol; m/e = 618 (M^+, 100%); UV–vis, 418 (380), 514 (17), 549 (7), 589 (6), 646 (4); NMR, pyrr 8.85 (8 H, s). *meso-Tri-3-pyridylphenylporphyrin* (*M3*): 50% acetone; m/e = 617 (M^+, 100%); UV–vis, 418 (400), 514 (18), 549 (8), 590 (6), 646 (4); NMR, pyrr 8.94 (2 H, d, J = 5), 8.85 (4 H, s), 8.81 (2 H, d, J = 5). *cis-meso-Di-3-pyridyldiphenylporphyrin* (*M2-cis*): 10% acetone; m/e = 617 (M^+ + 1, 100%); UV–vis, 418 (470), 514 (21), 549 (8), 590 (6), 646 (4); NMR, pyrr 8.90 (2 H, d, J = 5), 8.88 (2 H, s), 8.83 (2 H, s), 8.79 (2 H, d, J = 5). *trans-meso-Di-3-pyridyldiphenylporphyrin* (*M2-trans*): 5–10% acetone; m/e = 616 (M^+, 100%); UV–vis, 418 (470), 514 (20), 549 (8), 590 (6), 646 (4); NMR, pyrr 8.88 (4 H, d, J = 5), 8.79 (4 H, d, J = 5). *meso-3-Pyridyltriphenylporphyrin* (*M1*): 2% acetone; m/e = 615 (M^+, 100%); UV–vis, 418 (460), 514 (19), 549 (8), 590 (6), 646 (4); NMR, pyrr 8.91 (2 H, d, J = 5), 8.87 (4 H, s), 8.80 (2 H, d, J = 5).

meso-Tetra-2-pyridylporphyrin (*O4*): 5% methanol; m/e = 619 (M^+ + 1, 100%); UV–vis, 417 (400), 512 (18), 545 (6), 586 (5), 642 (3); NMR, pyrr 8.85 (8 H, s). *meso-Tri-2-pyridylphenylporphyrin* (*O3*): 50% acetone; m/e = 618 (M^+ + 1, 100%); UV–vis, 417 (400), 512 (20), 545 (4), 586 (3), 642 (2); NMR, pyrr 8.89 (8 H, m). *cis-meso-Di-2-pyridyldiphenylporphyrin* (*O2-cis*): 10–15% acetone; m/e = 617 (M^+ + 1, 100%); UV–vis, 417 (430), 512 (19), 548 (6), 588 (5), 650 (3); NMR, pyrr 8.95 (2 H, d, J = 5), 8.82 (2 H, s), 8.78 (2 H, s), 8.75 (2 H, d, J = 5). *trans-meso-Di-2-pyridyldiphenylporphyrin* (*O2-trans*): 5% acetone; m/e = 617 (M^+ + 1, 100%); UV–vis, 417 (450), 512 (19), 548 (6), 590 (6), 650 (3); NMR, pyrr 8.88 (4 H, d, J = 5), 8.82 (4 H, d, J = 5). *meso-2-Pyridyltriphenylporphyrin* (*O1*): CH_2Cl_2 alone; m/e = 616 (M^+ + 1, 100%); UV–vis, 417 (460), 512 (19), 548 (7), 588 (6), 650 (3); NMR, pyrr 8.8 (8 H, m).

Cationic Porphyrins. Quaternarizations of these porphyrins using methyl *p*-toluenesulfonate in refluxing dimethyl formamide for the P and M series (Pasternack et al., 1980; Hambrigth et al., 1976) and methyl iodide as alkylating agent and solvent for the O series (Hambrigth & Fleischer, 1970) led quantitatively to the corresponding cationic porphyrins, *meso*-(N-methyl-X-pyridiniumyl)$_n$(phenyl)$_{4-n}$$PH_2$. Substitution of their tosylate or iodide counterion by chloride was made by chromatography of all the water-soluble porphyrins using an ion-exchange Amberlite IRA-400 column. The cationic free base porphyrins were characterized by their mass (FAB technique), UV–visible (in H_2O), and ^{1}H NMR (in D_2O, CD_3OD, or CD_3OD–CD_2Cl_2) spectra, which were in good agreement with the proposed structures and also with literature data for the tetracationic derivatives (Pasternack et al., 1972; Kalyanasundaram, 1984; Shamim et al., 1979):

meso-Tetrakis(*N-methyl-4-pyridiniumyl*)*porphyrin* (*CH_3P_4*): m/e = 675 (M^+ − 3, 30%), 619 (M^+ + 1 − 4CH_3, 100%); UV–vis, 423 (220), 520 (14), 555 (5), 582 (6), 640 (2); NMR, *o*-Py 8.8 (8 H), *m*-Py 9.14 (8 H), pyrr 8.9 (8 H), CH_3 4.8 (12 H). *meso-Tris*(*N-methyl-4-pyridiniumyl*)*phenylporphyrin* (*CH_3P3*): m/e = 663 (M^+ + 1, 50%), 618 (M^+ + 1 − 3CH_3, 100%); UV–vis, 422 (200), 520 (14), 555 (6), 580 (6), 640 (2); NMR, *o*-Py 8.3 (6 H), *m*-Py 8.75 (6 H), *o*-Ph 8.2 (2 H), *m*- and *p*-Ph 7.8 (3 H), pyrr 8.85 (8 H), CH_3 4.8 (9 H). *trans-meso-Bis*(*N-methyl-4-pyridiniumyl*)*diphenylporphyrin* (*CH_3P2-trans*): m/e = 647 (M^+ + 1, 56%), 617 (M^+ + 1 − 2CH_3, 100%); UV–vis, 420 (240), 520 (8), 560 (6), 580 (5), 640 (2); NMR, *o*-Py 9.0 (4 H), *m*-Py 9.4 (4 H), *o*-Ph 8.3 (4 H), *m*- and *p*-Ph 7.9 (6 H), pyrr 8.9 (8 H), CH_3 4.8 (6 H). *cis-meso-Bis*(*N-methyl-4-pyridiniumyl*)*diphenylporphyrin* (*CH_3P2-cis*): m/e = 647 (M^+ + 1, 60%), 617 (M^+ + 1 − 2CH_3, 100%); UV–vis, 420 (140), 520 (7), 560 (5), 580 (4), 640 (2); NMR, *o*-Py 8.8 (4 H), *m*-Py 9.3 (4 H), *o*-Ph 8.2 (4 H), *m*- and *p*-Ph 7.8 (6 H), pyrr 8.9 (8 H), CH_3 4.8 (6 H).

meso-Tetrakis(*N-methyl-3-pyridiniumyl*)*porphyrin* (*CH_3M4*): m/e = 675 (M^+ − 3, 40%), 618 (M^+ − 4CH_3, 100%); UV–vis, 416 (250), 515 (19), 553 (4), 580 (4), 634 (1); NMR, 2-Py 9.96 (4 H), 4-Py 9.5 (4 H), 5-Py 8.57 (4 H), 6-Py 9.38 (4 H), pyrr 9.1 (8 H), CH_3 4.83 (12 H). *meso-Tris*(*N-methyl-3-pyridiniumyl*)*phenylporphyrin* (*CH_3M3*): m/e = 663 (M^+ + 1, 50%), 617 (M^+ − 3CH_3, 100%); UV–vis, 416 (280), 514 (16), 550 (4), 580 (6), 634 (2); NMR, 2-Py 9.96 (3 H), 4-Py 9.46 (3 H), 5-Py 8.57 (3 H), 6-Py 9.38 (3 H), *o*-Ph 8.24 (2 H), *m*- and *p*-Ph 7.88 (3 H), pyrr 9.11 (8 H), CH_3 4.81 (9 H). *trans-meso-Bis*(*N-methyl-3-pyridiniumyl*)*diphenylporphyrin* (*CH_3M2-trans*): m/e = 646 (M^+, 60%), 616 (M^+ − 2CH_3, 100%); UV–vis, 416 (310), 516 (15), 553 (5), 582 (6), 637 (3); NMR, 2-Py 9.94 (2 H), 4-Py 9.44 (2 H), 5-Py 8.56 (2 H), 6-Py 9.38 (2 H), *o*-Ph 8.24 (4 H), *m*- and *p*-Ph 7.88 (6 H), pyrr 9.04 (8 H), CH_3 4.76 (6 H). *cis-meso-Bis*(*N-methyl-3-pyridiniumyl*)*diphenylporphyrin* (*CH_3M2-cis*): m/e = 647 (M^+ + 1, 55%), 617 (M^+ + 1 − 2CH_3, 100%); UV–vis, 416 (300), 517 (18), 555 (6), 581 (7), 636 (3); NMR, 2-Py 9.93 (2 H), 4-Py 9.44 (2 H), 5-Py 8.56 (2 H), 6-Py 9.38 (2 H), *o*-Ph 8.22 (4 H), *m*- and *p*-Ph 7.84 (6 H), pyrr 9.02 (8 H), CH_3 4.77 (6 H).

Porphyrins O4, O3, O2-cis, and O2-trans should exist as a mixture of atropoisomers because of the lack of rotation of their *meso*-(*N*-methylpyridiniumyl) rings. This was the case

as shown by the complexity of the signals of their methyl protons. Therefore, the ^1H NMR signals of these porphyrins appeared as more complex and broader peaks. However, their integration was in good agreement with the proposed structure: Py 9.1–8.4, *o*-Ph 8.2, *m*- and *p*-Ph 7.7–7.8, pyrr 9.1–8.4, CH_3 3.8–4.2.

meso-Tetrakis(N-methyl-2-pyridiniumyl)porphyrin (CH₃O4): *m/e* = 675 ($M^+ - 3$, 30%), 662 ($M^+ - 1 - CH_3$), 619 ($M^+ + 1 - 4CH_3$, 100%); UV–vis, 418 (210), 512 (15), 545 (3), 582 (3), 634 (2).

meso-Tris(N-methyl-2-pyridiniumyl)phenylporphyrin (CH₃O3): *m/e* = 662 (M^+, 45%), 648 ($M^+ + 1 - CH_3$), 633 ($M^+ + 1 - 2CH_3$), 618 ($M^+ + 1 - 3CH_3$); UV–vis, 418 (250), 517 (10), 550 (sh), 580 (4), 640 (2). *trans-meso-Bis(N-methyl-2-pyridiniumyl)diphenylporphyrin (CH₃O2-trans)*: *m/e* = 647 ($M^+ + 1$, 55%), 631 ($M^+ - CH_3$), 617 ($M^+ + 1 - 2CH_3$, 100%); UV–vis, 418 (240), 517 (8), 550 (sh), 580 (4), 640 (2). *cis-meso-Bis(N-methyl-2-pyridiniumyl)diphenylporphyrin (CH₃O2-cis)*: *m/e* = 647 ($M^+ + 1$, 50%), 631 ($M^+ - CH_3$), 617 ($M^+ + 1 - 2CH_3$, 100%); UV–vis, 418 (210), 518 (8), 550 (3), 580 (4), 640 (2).

meso-Tris(N-methyl-4-pyridiniumyl)(2-methoxyphenyl)porphyrin (CH₃P3-OCH₃) was synthesized from *meso*-tri-4-pyridyl(2-methoxyphenyl)porphyrin (P3-OCH_3) according to Verlhac (1984): UV–vis, 420 (200), 512 (19), 545 (9), 585 (9), 630 (3); NMR (in DMSO-d_6) m-Py 9.6 (6 H, m), *o*-Py and pyrr 9–8.5 (14 H, m), *o*-Ph 7.7 (1 H, m), *p*-Ph 7.3 (1 H, t, *J* = 7), *m*-Ph (2 H, m), CH_3 4.85 (9 H, s), CH_3O 3.4 (3 H, s), NH −2.8 (2 H, s).

Copper(II) Porphyrins. According to Pasternack (Pasternack et al., 1975), 3×10^{-5} mol of a cationic porphyrin and 1.1 equiv of $CuCl_2$ were refluxed in water (or in an alcohol–water mixture) for 2 h. The color changed from violet to red (the end of the reaction was checked by UV–visible spectroscopy). After cooling, a few drops of a saturated solution of KI were added and the copper complex precipitated. After filtration, the porphyrin was dissolved in water (or in an alcohol–water mixture) and passed through an ion-exchange Amberlite IRA-400 column having chloride ions as counterions (60–70% yield). Copper porphyrins have been characterized by mass spectrometry and by UV–visible spectroscopy:

Cu-CH₃P4: *m/e* 739 (M^+, 50%), 724 ($M^+ - 1 - CH_3$), 710 ($M^+ - 1 - 2CH_3$), 694 ($M^+ - 3CH_3$); UV–vis, 424 (120), 547 (13), 580 (7). *Cu-CH₃P3*: *m/e* 724 ($M^+ + 1$, 70%), 709 ($M^+ + 1 - CH_3$), 695 ($M^+ + 2 - 2CH_3$); UV–vis, 424 (110), 547 (10), 580 (6). *Cu-CH₃P2-cis*: *m/e* 711 ($M^+ + 4$, 80%); UV–vis, 418 (140), 550 (14), 590 (9). *Cu-CH₃P2-trans*: *m/e* 711 ($M^+ + 4$, 80%); UV–vis, 418 (100), 550 (12), 590 (7).

Cu-CH₃M4: *m/e* 739 (M^+, 60%); UV–vis, 419 (230), 542 (16), 576 (4). *Cu-CH₃M3*: *m/e* 727 ($M^+ + 4$, 60%); UV–vis, 419 (250), 542 (12), 576 (4). *Cu-CH₃M2-cis*: *m/e* 711 ($M^+ + 4$, 55%); UV–vis, 417 (180), 546 (12), 586 (2). *Cu-CH₃M2-trans*: *m/e* 711 ($M^+ + 4$, 60%); UV–vis, 417 (200), 547 (11), 590 (2).

Chloroiron(III) Porphyrins. According to Pasternack et al. (1977), 500 equiv of $FeCl_2$ were added to 3×10^{-5} mol of a cationic porphyrin in water (or in an alcohol–water mixture). The mixture was refluxed overnight and the excess of iron was filtered. After addition of a few drops of a saturated solution of KI, the iron salt precipitated on cooling. After filtration, the porphyrin was dissolved in water (or in an alcohol–water mixture) and passed through an ion-exchange column (Chelex 100) to have chloride ions as counterions (40–50% yield). Chloroiron(III) porphyrins have been characterized by mass spectrometry. Their UV–visible spectra were dependent on the nature of the iron axial ligand in water solution.

Fe-CH₃P4: *m/e* 731 ($M^+ - 1$, 50%); UV–vis, 400, 570, 580. *Fe-CH₃P3*: *m/e* 719 ($M^+ + 3$, 75%); UV–vis, 398, 570, 630. *Fe-CH₃P2-cis*: *m/e* 703 ($M^+ + 3$, 70%); UV–vis, 400, 580, 620. *Fe-CH₃P2-trans*: *m/e* 703 ($M^+ + 3$, 70%); UV–vis, 417, 580, 620.

Fe-CH₃M4: *m/e* 731 ($M^+ - 1$, 55%); UV–vis, 417, 570, 640. *Fe-CH₃M3*: *m/e* 719 ($M^+ + 3$, 60%); UV–vis, 417, 570, 630. *Fe-CH₃M2-cis*: *m/e* 703 ($M^+ + 3$, 80%); UV–vis, 400, 570, 610. *Fe-CH₃M2-trans*: *m/e* 703 ($M^+ + 3$, 90%); UV–vis, 400, 570, 610.

Fe-CH₃O4: *m/e* 731 ($M^+ - 1$, 40%); UV–vis, 408, 590, 640. *Fe-CH₃O3*: *m/e* 719 ($M^+ + 3$, 55%); UV–vis, 408, 590, 640. *Fe-CH₃O2-cis*: *m/e* 703 ($M^+ + 3$, 70%); UV–vis, 408, 594, 630. *Fe-CH₃O2-trans*: *m/e* 703 ($M^+ + 3$, 70%); UV–vis, 408, 590, 640.

Physical Measurements. (*A*) *^1H NMR.* Spectra were recorded, at 20 °C, on a Brucker WM 250 spectrometer operating at 250 MHz FT in $CDCl_3$. Chemicals shifts are reported in ppm downfield from $(CH_3)_4Si$, with *J* in Hz (s, d, t, and m were used for singlet, doublet, triplet, and multiplet).

(*B*) *Mass Spectrometry.* Mass spectra were recorded on a RIBER R1010 mass spectrometer coupled with a PDP8 computer or VG70-250 double-focusing instrument equipped with a fast atom bombardment gun, operating with xenon at 7.5 kV and 1.2 mA. The scanning acquisition parameters were as follows: accelerating voltage, 4 kV; scan time, 15 s/decade; interscan time, 2 s. The apparatus was calibrated with cesium iodide, and different matrices were used: glycerol, thioglycerol, and dimethyl sulfoxide.

(*C*) *UV–Visible Spectroscopy.* UV–visible absorption spectra of porphyrins were recorded in the 360–700-nm range on a Uvikon 820 (Kontron) spectrophotometer. Titration of porphyrins (20 μM in 0.1 M Tris-HCl buffer, pH 7.4, containing 0.1 M NaCl) by concentrated solutions of CT DNA was done, at 25 °C, until a final concentration of 500 μM DNA base pairs was reached (final [porphyrin]:[DNA base pairs] ratio, r_f, = 0.04).

(*D*) *Fluorescence Spectroscopy.* Fluorescence excitation (350–600-nm range with a λ_{em} = 640 nm) and emission (500–800-nm range with a λ_{ex} = 420 nm) spectra of porphyrins (2 μM), either free or bound to CT DNA (r_f = 0.1) in 0.2 cm wide quartz cuvettes in order to minimize the inner-filter effect, were recorded on a photon-counting spectrofluorometer, SLM 800, associated to a MINC Digital computer.

(*E*) *Fluorescence Energy Transfer.* Contact energy transfer from the nucleic acid bases to the bound porphyrin was measured from fluorescence excitation spectra recorded between 240 and 350 nm, every 2 nm (λ_{em} = 650 nm) with a yellow filter at the emission (to eliminate second-order spectra). A correcting factor for each point of the excitation spectra was calculated by comparison of the UV–visible absorption (1 μM porphyrin) and fluorescence excitation (0.1 μM porphyrin) spectra of porphyrins. The ratio between the quantum yield of the bound porphyrin with excitation in the UV spectral region of nucleic acids (Q_λ) versus excitation at 310 nm (Q_{310}) was calculated according to Le Pecq and Paoletti (1967) by using

$$\frac{Q_\lambda}{Q_{310}} = \left(\frac{I_\lambda}{I_{310}}\frac{\epsilon_{310}}{\epsilon_\lambda}\right)_b \left(\frac{I_{310}}{I_\lambda}\frac{\epsilon_\lambda}{\epsilon_{310}}\right)_f \quad (1)$$

where *I* and ε are respectively the measured fluorescence intensity and molar extinction coefficients of free (f) and bound (b) porphyrin (r_f = 0.1). λ = 310 nm was chosen as normalization wavelength because of the very low absorption of

nucleic acids in this region of the spectrum.

(*F*) *Viscosimetric Titration.* Viscosimetric measurements of the length increase of the short helices of sonicated DNA were performed according to Saucier et al. (1971) in a semimicrodilution capillary viscosimeter (Cannon Instrument Corp.) mounted in a high-precision temperature-regulated bath (20 °C). Flow times were measured ($t \pm 0.1$ ms) by the use of photoelectric sensors and an electronic timer. All the solutions were filtered on Sep-Pak C18 before use. Sonicated DNA (1.4 mL, 300 μM bp) was introduced in the viscosimeter, and concentrated solutions of porphyrins (400 μM) were added in successive 10-μL aliquots. log (η/η_0) was plotted against log $(1 + 2r)$, η_0 and η being the intrinsic viscosity of the DNA in the absence and in the presence of porphyrins, respectively, and r being the [bound porphyrin]:[DNA base pairs] ratio.

(*G*) *Apparent Binding Constant Measurements.* Apparent binding constants were measured by competition with EB. This assay takes advantage of the fluorescence properties of EB when it is intercalated into CT DNA and consists of the measurement of the fluorescence intensity of EB bound to CT DNA in the presence of various concentrations of the studied competitor. Four quartz Hellma cuvettes (3 mL) were used for the experiments: the first one was filled with 3 mL of buffer, the second with 3 mL of CT DNA (final concentration 2 μg/mL), the third with a 3-mL solution containing CT DNA (2 μg/mL) and the studied porphyrin at a final concentration ranging from 0.5 to 5 μM (several concentrations of each porphyrin were tested until EB displacement was observed), and the fourth with the same amount of DNA and double the amount of porphyrin. EB (100 μg/mL) was then progressively added in successive 10-μL aliquots in each cuvette and its binding to DNA recorded at 540 nm for excitation and 610 nm for emission. The decrease of fluorescence in the cuvettes containing porphyrins allowed the determination of the apparent binding constants (K_{app}) of the porphyrin to CT DNA according to Le Pecq and Paoletti (1967). The binding constant of EB for DNA in the experimental conditions was 2×10^5 M^{-1}.

Ultrapure water was obtained through a reverse osmosis system (Elga, Millipore). All experiments with water-soluble porphyrins and EB with DNA were performed in 0.1 M Tris-HCl buffer, pH 7.4, containing 0.1 M NaCl, at 25 °C.

Results

Preparation and Characterization of and Abbreviations for the Porphyrins and Metalloporphyrins Studied. Porphyrins corresponding to the general formula *meso*-(4-pyridyl)$_n$(phenyl)$_{4-n}$PH$_2$ were prepared by condensastion of pyrrole with a mixture of benzaldehyde and 4-pyridinecarboxaldehyde (see Materials and Methods). This reaction led to a mixture of six porphyrins (Figure 1). The five porphyrins formed in addition to *meso*-tetraphenylporphyrin were named as indicated in Table I: P4, P3, P2-cis, P2-trans, and P1. P was used to indicate that the nitrogen atom of the *meso*-pyridyl rings was in the para position, and the indicated number referred to the number of *meso*-pyridyl rings in the molecule. Porphyrins corresponding to the general formula *meso*-[3(or 2)-pyridyl]$_n$(phenyl)$_{4-n}$PH$_2$ were obtained by identical methods using 3- or 2-pyridinecarboxaldehyde and were called M4, M3, M2-cis, M2-trans, and M1 for those having *meso*-(*m*-N)-pyridyl groups and O4, O3, O2-cis, O2-trans, and O1 for those having *meso*-(*o*-N)pyridyl groups. All these porphyrins were characterized by UV–visible and ^{1}H NMR spectroscopy and by mass spectrometry (see Materials and Methods). Our results were in good agreement with the literature data reported for the porphyrins previously described: P4, P3, P2-cis and -trans, and P1 (Shamin et al., 1981) and M4 and O4 (Kalyanasundaram, 1984).

Table I: Interactions of Various Porphyrins and Metalloporphyrins with CT DNA:Hypochromic Effects and Apparent Binding Constants

	free bases		copper complexes		iron complexes	
porphyrins	H^a	$K_{app}{}^b$	H	K_{app}	H	K_{app}
CH_3P4	40	1000 ± 200	20	1200 ± 300	−10	60 ± 10
CH_3P_3	30	300 ± 80	20	330 ± 80	−5	23 ± 5
CH_3P2-cis	25	120 ± 30	20	140 ± 30	0	8 ± 2
CH_3P2-trans	25	140 ± 40	20	150 ± 40	−5	8 ± 2
CH_3M4	30	160 ± 30	20	180 ± 30	−10	60 ± 10
CH_3M3	25	50 ± 10	20	60 ± 15	0	23 ± 5
CH_3M2-cis	25	18 ± 3	15	21 ± 5	−10	8 ± 2
CH_3M2-trans	25	16 ± 4	20	22 ± 6	−10	8 ± 2
CH_3O4	<10	40 ± 6			10	50 ± 10
CH_3O3	<10	16 ± 2			5	18 ± 4
CH_3O2-cis	25	9 ± 2			0	6 ± 2
CH_3O2-trans	<10	5 ± 1			10	6 ± 2
CH_3P3-OCH_3	30	50 ± 10				

[a] H = % decrease of the Soret peak of the porphyrin (20 μM) in 0.1 M Tris-HCl buffer, pH 7.4, containing NaCl, 0.1 M at 25 °C, in the presence of CT DNA (500 μM base pairs). Under these conditions, the initial positions of the Soret peak (before CT DNA addition) were 422 (CH_3P4), 422 (CH_3P3), 417 (CH_3P2-cis), 418 (CH_3P2-trans), 417 (CH_3M4), 418 (CH_3M3), 416 (CH_3M2-cis), 416 (CH_3M2-trans), 414 (CH_3O4), 416 (CH_3O3), 417 (CH_3O2-cis), 413 (CH_3O2-trans), and 420 (CH_3P3-OCH_3) for the free base porphyrins and 424 (Cu-CH_3P4 and Cu-CH_3P3), 419 (Cu-CH_3M4 and Cu-CH_3M3), 418 (Cu-CH_3P2-cis and Cu-CH_3P2-trans), and 417 (Cu-CH_3M2-cis and Cu-CH_3M2-trans) for the Cu(II) complexes. Upon addition of 500 μM CT DNA, red shifts of those peaks (between 8 nm for CH_3P4 and 2 nm for CH_3P2-cis) were observed for all the porphyrins or Cu(II)–porphyrins that gave a significant hypochromic effect (>15% decrease of the Soret peak). None of the used iron–porphyrin complexes gave significant hypochromic effect. [b] Apparent binding constants, in 10^{-4} M^{-1}, for CT DNA in 0.1 M Tris-HCl buffer, pH 7.4, containing 0.1 M NaCl, at 25 °C (conditions under Materials and Methods). Mean values ± SD for four to eight determinations.

The corresponding cationic porphyrins were prepared by methylation of the pyridine nitrogens, obtained as chloride salts and characterized by UV–visible and ^{1}H NMR spectroscopy and by mass spectrometry. Their abbreviations were deduced from those of their pyridyl precursors by simple addition of CH_3 (for instance, CH_3P4 is derived from P4).

From the 15 prepared cationic porphyrins (Table I), those of the CH_3P and CH_3M series can temporarily adopt planar conformations as all their pyridiniumyl rings can freely rotate. The four *meso*-pyridiniumyl rings of porphyrin CH_3O4 cannot rotate, and in the same way, three, two, and one *meso*-pyridiniumyl groups of porphyrins CH_3O3, CH_3O2 (cis and trans), and CH_3O1 cannot rotate, respectively. It was interesting to compare the mode of binding to DNA of these five porphyrins having more or less large areas that can be temporarily planar. Unfortunately, CH_3O1, as well as the two other monocationic porphyrins CH_3P1 and CH_3M1, were found too insoluble in water for binding studies. Therefore, we prepared a cationic porphyrin that contained, as does CH_3O1, only one nonrotating *meso*-aryl group, but which was much more soluble in water. This porphyrin, *meso*-tris(*N*-methyl-4-pyridiniumyl)(2-methoxyphenyl)porphyrin (CH_3P3-OCH_3), was sufficiently soluble in water because of its three positive charges and involved only one meso group which cannot rotate. It was prepared by methylation of *meso*-tri-4-pyridyl(2-methoxyphenyl)porphyrin, ($P3$-OCH_3), which was obtained as previously described (Verlhac, 1984).

The Cu^{II} and $ClFe^{III}$ complexes of the cationic porphyrins were prepared by standard procedures (Pasternack et al., 1975,

1977) and characterized by UV–visible spectroscopy and by mass spectrometry (see Materials and Methods).

Study of the Mode of Binding between Porphyrins and CT DNA. (A) UV–Visible Study. UV titrations were performed with all the porphyrins (10 μM) in solutions containing an increasing concentration of CT DNA as previously described (Fiel et al., 1979; Pasternack et al., 1983a). Interaction of CT DNA with all the porphyrins of the CH_3P and CH_3M series as well as with their Cu(II) complexes led to characteristics very similar to those previously reported for CH_3P4 and CH_3M4: a bathochromic shift of their Soret peak and a strong hypochromic effect (up to 40% decrease of the Soret peak, as a function of the ionic strength and the [porphyrin]:[DNA base pairs] ratio = r). Table I compares the hypochromic effects observed for all porphyrins or metalloporphyrins under identical conditions of moderate ionic strength (μ = 0.2 M) and large excess of CT DNA base pairs relative to porphyrin (r = 0.04). All the porphyrins of the CH_3P and CH_3M series exhibited clear hypochromic effects (decrease of the Soret peak between 25 and 40%) under these conditions. Interestingly, CH_3P3-OCH_3 and CH_3O2-cis, which bear respectively one and two meso substituents that cannot rotate, also exhibit similar bathochromic and hypochromic effects. On the contrary, the other porphyrins of the CH_3O series, including CH_3O2-trans, CH_3O3, and CH_3O4, gave no significant perturbation of their UV–visible spectra upon titration with CT DNA. All the studied Fe(III) complexes exhibited no change of their spectra upon titration with CT DNA (Table I).

(B) Fluorescence Spectra. Fluorescence excitation and emission spectra were recorded in the absence or presence of DNA for all the free base porphyrins. In the absence of CT DNA, all porphyrins presented an excitation spectrum with a maximum at 420 nm and an emission spectrum with a maximum around 650–660 nm (Figure 3). In the presence of CT DNA, a decrease (around 50%) of the intensity of both the excitation and emission spectra was observed for all the porphyrins of the CH_3P and CH_3M series as well as for CH_3O2-cis and CH_3P3-OCH_3 porphyrins (Figure 3). On the contrary, there was no major effect of CT DNA on the spectra of the other porphyrins of the CH_3O series, such as CH_3O4, CH_3O3 or CH_3O2-trans.

(C) Energy-Transfer Experiments. From a comparison of the fluorescence excitation spectra of CH_3P4, either free or bound to CT DNA, and of the corresponding absorption spectra, it has been shown that the fluorescence quantum yield of CH_3P4 increased by a factor of 2–3 for an excitation wavelength around 260 nm when it was bound to DNA (Sari et al., 1986). A similar phenomenon, which is due to transfer of the energy absorbed by DNA (at 260 nm) to the porphyrin, has been previously found for ethidium bromide and several other intercalating agents (Le Pecq & Paoletti, 1967; Reinhardt et al., 1982). The energy transfer has been considered as evidence for intercalation as it could be calculated that such an energy transfer could only occur if a close contact existed between the intercalating agent and DNA base pairs according to the Forster equation (Reinhardt et al., 1982).

Such energy-transfer experiments were performed with all the free base porphyrins studied, and the results are given in Figure 4. All the porphyrins of the CH_3P series led to a clear increase of fluorescence quantum yields by a factor varying from 2 for CH_3P4 to 3.6 for CH_3P2-cis. Very similar results were obtained for the porphyrins of the CH_3M series. On the contrary, all the porphyrins of the CH_3O series failed to give any increase of fluorescence quantum yield upon excitation between 240 and 350 nm, except for CH_3O2-cis, for which a 4-fold increase was observed (Figure 4). Interestingly, the CH_3P3-OCH_3 porphyrin gave a result almost identical with that for CH_3O2-cis.

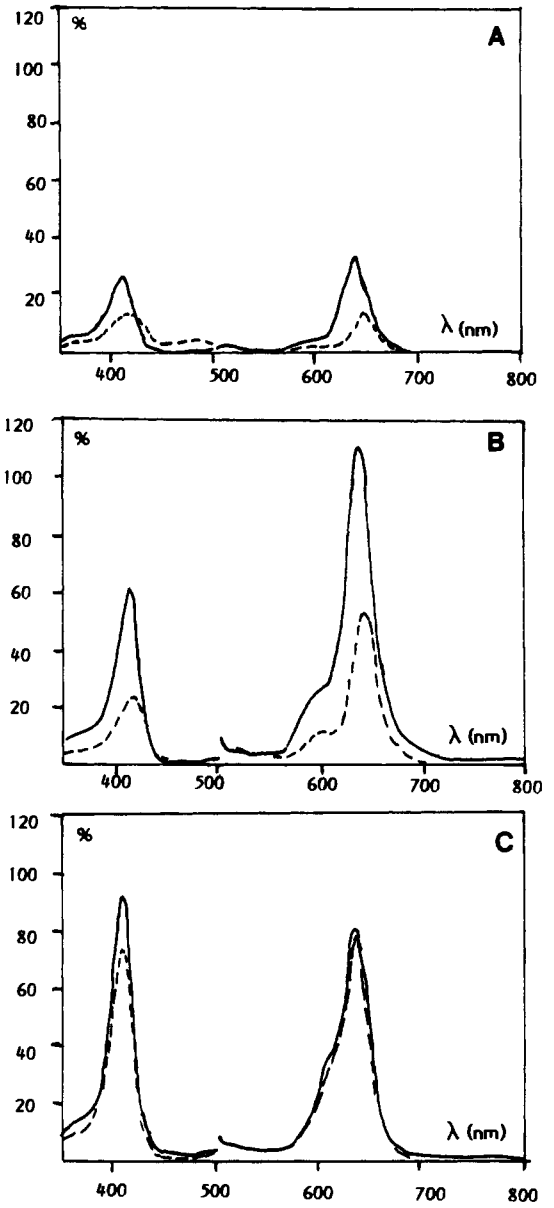

FIGURE 3: Fluorescence excitation and emission spectra of selected porphyrins: CH_3M2-cis (A), CH_3O2-cis (B), and CH_3O2-trans (C); (—) in the absence of CT DNA and (---) in the presence of CT DNA. Excitation spectra between 350 and 500 nm with a λ emitted = 640 nm; emission spectra between 500 and 800 nm with a λ excitation = 420 nm. Conditions: 2 μM porphyrin and 20 μM CT DNA base pairs in 0.1 M Tris-HCl buffer, pH 7.4, containing 0.1 M NaCl, at 25 °C.

(D) Viscosimetry. Viscosimetric measurements of the lengthening of sonicated DNA were performed according to Saucier et al. (1971). A curve characteristic of each porphyrin was obtained by plotting log (η/η_0) as a function of log $(1 + 2r)$, η and η_0 being the intrinsic viscosity of DNA either in the presence or in the absence of porphyrin and r being the [bound porphyrin]:[DNA base pair] ratio. EB was also studied as a reference compound (Figure 5). As previously reported (Saucier et al., 1971), this classical intercalating agent gave a straight line with a slope of 2 as expected since the intercalation of one molecule into DNA results in an increase of DNA length, corresponding formally to the addition of a base pair per DNA molecule.

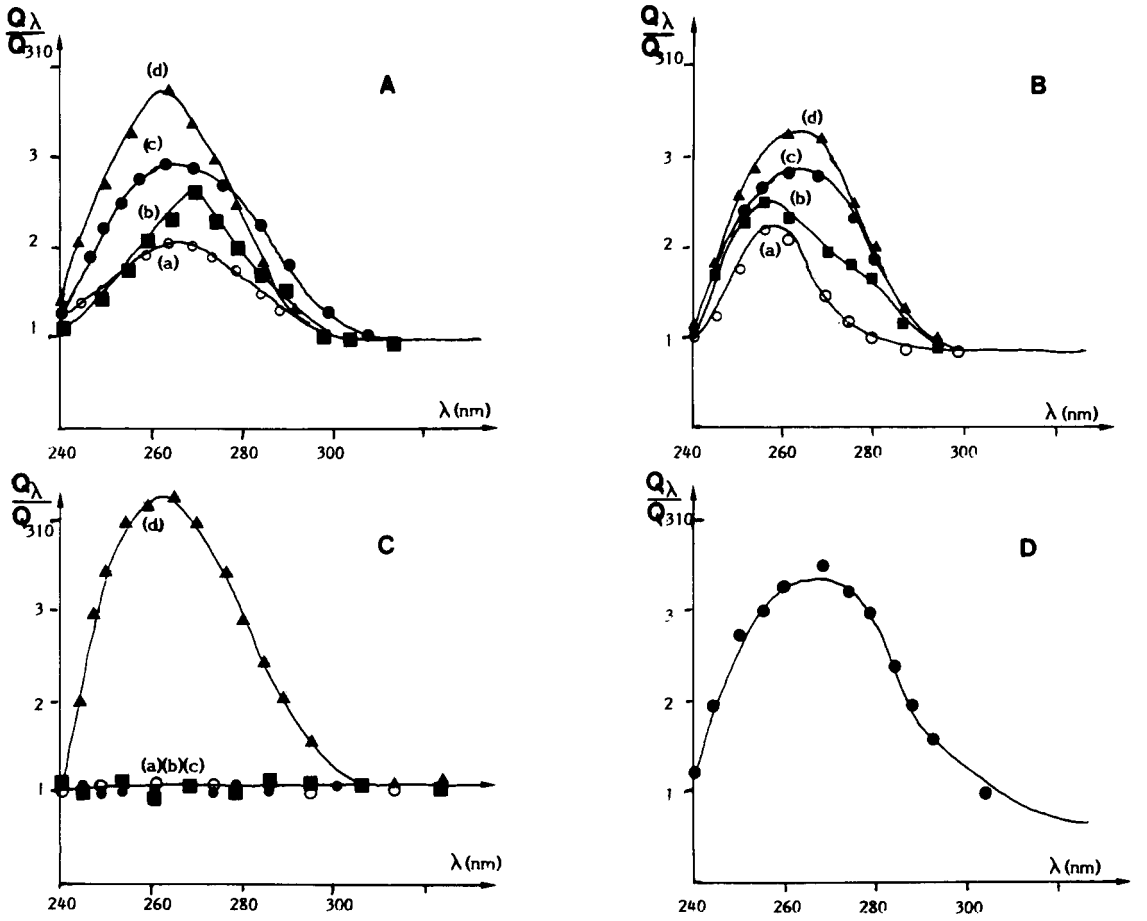

FIGURE 4: Variation of the fluorescence quantum yield of different porphyrins in the presence of CT DNA as a function of the excitation wavelength. (A) CH_3P4 (a), CH_3P3 (b), CH_3P2-trans (c), CH_2P2-cis (d); (B) CH_3M4 (a), CH_3M3 (b), CH_3M2-trans (c), CH_3M2-cis (d); (C) CH_3O4 (a), CH_3O3 (b), CH_3O2-trans (c), CH_3O2-cis (d); (D) CH_3P3-OCH_3. The ratio of the fluorescence quantum yield at λ (Q_λ) to the fluorescence quantum yield at 310 nm (Q_{310}) for the different porphyrins bound to CT DNA was computed from their fluorescence excitation spectra (recorded at 660 nm) and absorption spectra in the presence or absence of CT DNA (conditions as in Figure 3; see Materials and Methods).

CH_3P4 led to a straight line with a slope of about 1.6 instead of 2, indicating a smaller increase of DNA length than with EB itself. This result was in agreement with those previously reported (Fiel et al., 1979). However, in order to know whether or not this smaller value of the slope obtained with CH_3P4 was evidence against the intercalation of this porphyrin, we have measured the DNA lengthening by another method using electron microscopy as described previously (Butour et al., 1978). This method used circulary nicked DNA, the size of which was measured in the presence or absence of porphyrins by use of electron microscopy. A 50% increase in length relative to the control was observed in the presence of an excess of CH_3P4 as well as of EB (data not shown). This result showed that the slightly smaller increase of the slope observed for CH_3P4 than for EB in viscosimetry measurements was not indicative of an absence of intercalation of this compound into DNA.

All the porphyrins of the CH_3P and CH_3M series, as well as their Cu(II) complexes, led to DNA lengthening with slopes of $\log (\eta/\eta_0) = f[\log (1 + 2r)]$ straight lines between 1.5 and 1.65. Porphyrin CH_3O2-cis caused also a lengthening of DNA with a slope of 1.13 whereas CH_3O4, CH_3O3, CH_3O2-trans, and all ferric porphyrins failed to induce any change of DNA length.

Determination of Apparent Affinity Binding Constants. UV-visible titration has been used to determine the apparent affinity binding constant (K_{app}) of CH_3P4 and CH_3M4 for CT DNA (Fiel et al., 1979; Dougherty et al., 1985). Nevertheless, this method has two severe limitations: (i) it is very difficult to determine the absorption coefficient of the bound porphyrin (Pasternack et al., 1983a; Strickland et al., 1988), and (ii) it is only applicable to intercalating porphyrins for which the Soret peak is greatly modified upon binding to DNA.

K_{app} measurements were performed as described by Le Pecq and Paoletti for other compounds (Le Pecq & Paoletti, 1967). This method uses the competition between EB and the studied compound for binding to DNA and measures the decrease of fluorescence of EB bound to DNA in the presence of the compound to be studied. This method can be used for all compounds having a good affinity for DNA whatever their mode of binding may be as it only measures the ability of a compound to prevent intercalation of EB into DNA. First, we have checked that the decrease of fluorescence of EB bound to DNA in the presence of porphyrins was due to the release of bound EB and not to a quenching of its fluorescence by porphyrins. For that, we showed that no significant energy transfer occurred between EB and CH_3P4 by measurement of the porphyrin fluorescence in the presence of EB after an excitation at 540 nm. Moreover, a tetraanionic porphyrin, *meso*-tetrakis(4-sulfonatophenyl)porphyrin, which had no affinity for CT DNA, did not change the fluorescence of EB bound to DNA, even at concentrations up to 10 μM, which were much higher than those used in our experiments.

K_{app} values obtained for the various studied porphyrins or metalloporphyrins are given in Table I and Figure 5. These K_{app} varied from 1.2×10^7 to 5×10^4 M^{-1}. All the determinations of K_{app} were done for an identical ionic strength (μ = 0.2 M) which has been previously used by Fiel et al. (1979)

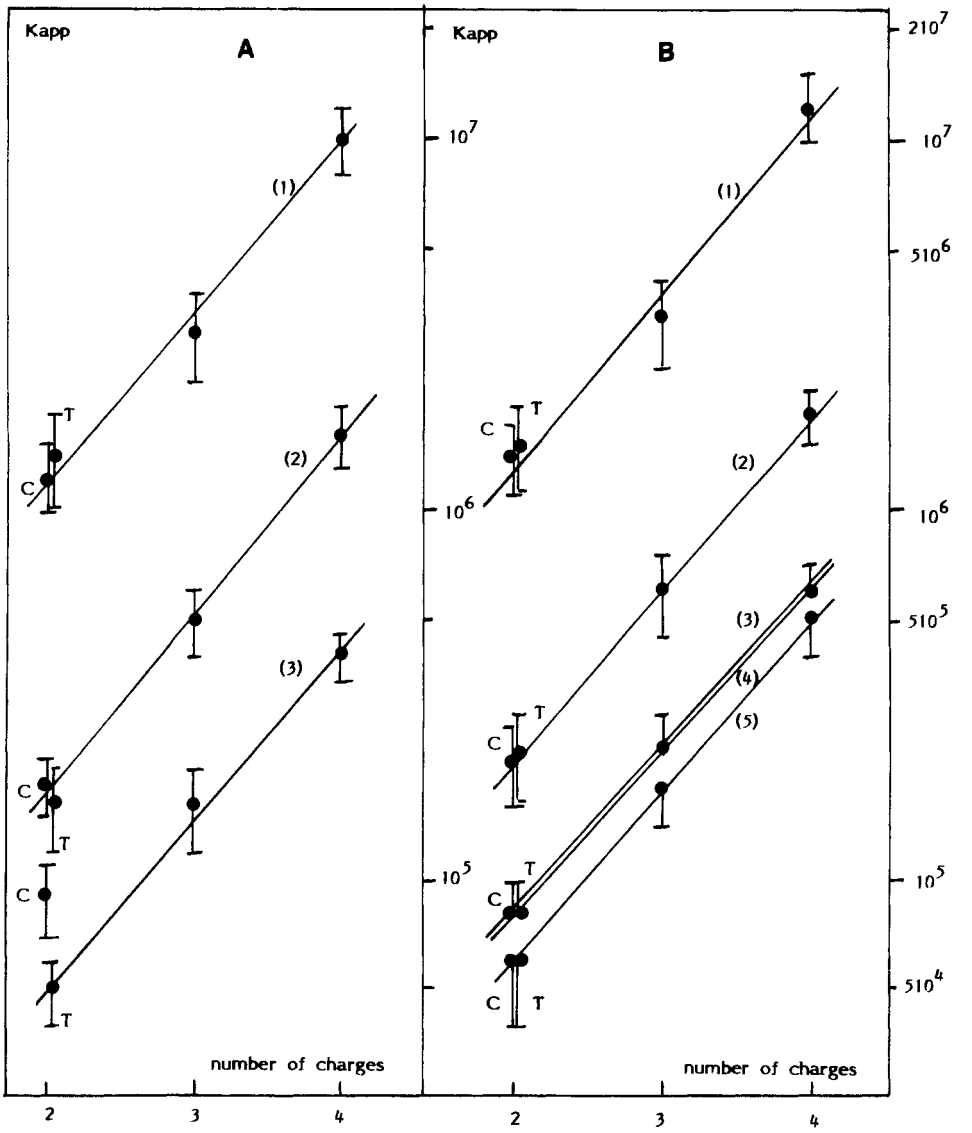

FIGURE 5: Relationship between log K_{app} of various cationic free base porphyrins (A) and of their Cu(II) and Fe(III) complexes (B) with their charge number. (A) CH_3P series (1), CH_3M series (2), CH_3O series (3); (B) Cu-CH_3P series (1), Cu-CH_3M series (2), Fe-CH_3P series (3), Fe-CH_3M series (4), Fe-CH_3O series (5). C for cis and T for trans; data from Table I.

to determine the K_{app} of CH_3P4 for CT DNA by UV–visible titration. The K_{app} values obtained by this technique for CH_3P4 and CH_3M4 (Fiel et al., 1979; Dougherty et al., 1985) are similar to those obtained by competition binding with EB. As previously reported in the case of CH_3P4 and CH_3M4 (Dougherty et al., 1985), the K_{app} listed in Table I varied with the ionic strength of the medium. For instance, K_{app} of CH_3P3 varied from 3×10^6 to 1.2×10^7 M^{-1} when the ionic strength decreased from 0.2 to 0.02 M.

As far as nonintercalating porphyrins such as CH_3O4 are concerned, it is not possible to compare their binding constants determined by our approximate EB-displacement method to literature values obtained by other techniques. Actually, there are so far no data in the literature about binding constants of nonintercalating porphyrins with CT DNA itself. Available data concern binding constants of Zn-CH_3P4 (Strickland et al., 1988), Cu-CH_3O4, and CH_3O4 (Strickland et al., 1989) to polynucleotides measured by the equilibrium dialysis technique. It is noteworthy that the values obtained by this technique for the binding constants of these nonintercalating porphyrins to poly[d(AT)]$_2$ are lower than those of the corresponding intercalating porphyrins but still remain between 10^5 and 10^6 M^{-1}. This is also in agreement with our data determined by the EB-displacement method.

As shown in Figure 5A, inside a given series (CH_3P, CH_3M, or CH_3O), log K_{app} increased in a linear manner as a function of the number of the cationic charges of the porphyrin. The loss of one charge corresponded to a 3-fold decrease of K_{app}. As far as the position of the pyridine nitrogen atom is concerned, porphyrins of the CH_3P series exhibited K_{app} 6 times higher than those of the CH_3M series and about 20 times higher than those of the CH_3O series having the same charge number. Cis and trans dicationic porphyrins of the CH_3P and CH_3M series had very similar K_{app} and were on the straight lines log $K_{app} = f$(number of charges) (Figure 5). On the contrary, CH_3O2-cis and CH_3O2-trans showed different K_{app} for CT DNA, only CH_3O2-cis being not on the correlation line of the CH_3O series. Finally, the K_{app} of CH_3P3-OCH_3 was found similar to that of the tricationic porphyrin CH_3M3 and much smaller than that of CH_3P3 (5×10^5, 5×10^5, and 3×10^6 M^{-1}, respectively).

For metalloporphyrins as for free base porphyrins, log K_{app} increased in a linear manner with the number of positive charges whatever the nature of the metal and of the position of the pyridine nitrogen atom (Figure 5B). Here too, the loss of one cationic charge resulted in a decrease of K_{app} by a factor about 3. However, whereas the K_{app} values of Cu(II)–porphyrins were almost identical with those of their corre-

sponding free base and were very dependent on the position of the *N*-methyl groups of the *meso*-pyridiniumyl substituents ($CH_3P > CH_3M > CH_3O$), K_{app} values of Fe(III)–porphyrins were much lower [between 6×10^5 and 6×10^4 M^{-1} instead of 1.2×10^7 to 2×10^5 M^{-1} for Cu(II)–porphyrins] and were almost independent of the position the *N*-methyl groups of the *meso*-pyridiniumyl substituents. As shown in Figure 5B, the straight lines for log K_{app} = *f*(number of charges) corresponding to the Fe(III)–porphyrins of the CH_3P and CH_3M series were superimposed and those corresponding to the CH_3O series were very close to the former ones. Finally, it is noteworthy that contrary to CH_3O2-cis and CH_3O2-trans, which showed different K_{app}s, their Fe(III) complexes exhibited identical K_{app}s.

Discussion

The technique that we have used to compare the affinities of various porphyrins and metalloporphyrins for CT DNA gave only a global apparent binding constant (K_{app}) irrespective of their mode of binding to DNA. In fact, K_{app} reported in Table I are only related to the ability of the porphyrins to prevent the binding of EB to DNA. Whatever their mode of binding to DNA may be, all the studied porphyrins and metalloporphyrins had in common the following characteristics: (i) a relatively high affinity for CT DNA at moderate ionic strength (μ = 0.2 M) with K_{app} values between 1.2×10^7 and 5×10^4 M^{-1} and (ii) a linear decrease of log K_{app} with the number of positive charges of the porphyrin ring, with a slope almost equal for all series of porphyrins or metalloporphyrins having the same metal ion (or absence of metal ion) and the same position of the *N*-methyl group of the *meso*-pyridiniumyl substituents (P, M, or O):

$$K_{app}(n \text{ charges}) \simeq 3K_{app}(n - 1 \text{ charges}) \qquad (2)$$

Remarkably, this was found to be true for all the following series: CH_3P, CH_3M, CH_3O (except for CH_3O2-cis), Cu(II)-CH_3P, Cu(II)-CH_3M, Fe(III)-CH_3P, Fe(III)-CH_3M, and Fe(III)-CH_3O.

For a given number of positive charges of the porphyrin, the binding affinity was found to be critically dependent on the position of the *N*-methyl group of pyridiniumyl rings and on the nature of the central metal ion (Table I and Figure 5). This should be related to their mode of binding to CT DNA. In fact, three types of binding of porphyrins to DNA have been described so far in the literature. *Intercalation* into DNA base pairs was shown for CH_3P4 and CH_3M4 by using many techniques (see the introduction) and, as far as the techniques used in this study are concerned, is characterized by (i) a red shift (about 10 nm) and decrease (up to 40%) of the porphyrin Soret peak in UV–vis spectroscopy, (ii) a clear decrease of the intensity of its fluorescence emission and excitation spectra, (iii) a 2- to 4-fold increase of its fluorescence quantum yield for an excitation around 260 nm corresponding to an energy transfer between DNA and the porphyrin, (iv) a lengthening of DNA, and (v) a relatively high binding constant for CT DNA (10^6–10^7 M^{-1}). *External groove binding* was indicated for porphyrins or metalloporphyrins that cannot exist, even temporarily, in a completely planar conformation, such as Fe(III)–porphyrins or CH_3O4. This binding is characterized by very different properties: (i) no (or minor) changes of the UV–visible spectra of the porphyrins, (ii) no (or minor) changes of the fluorescence spectra of the porphyrins, (iii) no energy transfer between DNA and porphyrin, (iv) no lengthening of DNA, and (v) a relatively low K_{app} for CT DNA ($\sim 5 \times 10^5$ M^{-1} for a tetracationic species). Very recently, *another mode of external binding* to polynucleotides or DNA was proposed for the dicationic porphyrins CH_3P2-cis and CH_3P2-trans on the basis of UV–visible and circular dichroism spectrocospy (Gibbs et al., 1988b). Especially at high ionic strength, these porphyrins appeared to bind externally to form long-range stacked structures on the exterior of nucleic acids. This interaction is characterized by a red shift and decrease of the porphyrin Soret peak as found for intercalating porphyrins. In fact, the nature of the binding of a possibly intercalating porphyrin to a polynucleotide or to DNA appears dependent on the nature of the polynucleotide sequence, the charge of the porphyrin, and the ionic strength of the medium (Fiel et al., 1979; Dougherty et al., 1985).

Table II: Compared Data Concerning the Interaction of Various Porphyrins and Metalloporphyrins with CT DNA

porphyrins	hypochromic effect on the Soret peak[a]	fluorescence decrease[b]	energy transfer[c]	DNA lengthening[d]
CH_3P4	+ (40)	+	+ (2.0)	+
CH_3M4	+ (30)	+	+ (2.2)	+
CH_3P3	+ (30)	+	+ (2.6)	+
CH_3M3	+ (25)	+	+ (2.5)	+
CH_3P2-cis	+ (25)	+	+ (3.6)	+
CH_3P2-trans	+ (25)	+	+ (2.9)	+
CH_3M2-cis	+ (25)	+	+ (3.3)	+
CH_3M2-trans	+ (25)	+	+ (2.9)	+
CH_3O2-cis	+ (25)	+	+ (3.2)	+
CH_3P3-OCH_3	+ (30)	+	+ (3.3)	+
CH_3O4	− (<10)	−	−	−
CH_3O3	− (<10)	−	−	−
CH_3O2-trans	− (<10)	−	−	−
Fe complexes[e]	− (−10 to 0)			−
Cu complexes[e]	+ (15 to 20)			+

[a] From data of Table I: (+) % decrease of the Soret peak in the presence of CT DNA >15%; (−) % decrease <10%; values indicated in parentheses. [b] (+) More than 50% decrease of fluorescence spectra in the presence of CT DNA (conditions of Figure 3); (−) no significant decrease. [c] (+) Existence of an energy transfer between CT DNA and porphyrins with a quantum yield increase between 2 and 4 as indicated in parentheses (conditions of Figure 4); (−) no energy transfer. [d] (+) Slope of the log $(\eta/\eta_0) = f[\log(1 + 2r)] > 1.1$ (values between 1.13 for CH_3O2-cis and 1.6 for CH_3P4 and between 1.5 and 1.65 for the Cu complexes); (−) no lengthening observed by viscosimetry. [e] For all complexes mentioned in Table I.

In order to determine the mode of binding to CT DNA of the various prepared porphyrins, we have compared in Table II their ability to satisfy the criteria previously proposed for intercalation—i.e., the existence (i) of a red shift and decrease of their Soret peak, (ii) of a decrease of the intensity of their fluorescence emission and excitation spectra, (iii) of an energy transfer from DNA to porphyrin upon irradiation around 260 nm (quantum yield increase > 2), and (iv) of a lengthening of DNA [slope of log $(\eta/\eta_0) = f[\log(1 + 2r)] > 1.1$].

Table II shows that all porphyrins of the CH_3P and CH_3M series, which can exist temporarily in a completely planar conformation, satisfied the four previous criteria. On the contrary, porphyrins CH_3O4, CH_3O3, and CH_3O2-trans, which involve 4, 3, or 2 nonrotating *meso*-aryl groups, did not satisfy any of these criteria. Porphyrins CH_3O2-cis and CH_3P3-OCH_3, which involve respectively two and one nonrotating *meso*-aryl groups, both satisfied the four intercalation criteria. These data suggest that all the porphyrins which can exist at least temporarily in a completely planar conformation, such as those of the CH_3P and CH_3M series, as well as their Cu(II) complexes, are intercalated into CT DNA under the conditions used in this study. These porphyrins and their Cu(II) complexes exhibit high affinity for CT DNA with log K_{app} varying linearly with the number of positive charges and K_{app} higher for the CH_3P than for the CH_3M series.

On the contrary, all the porphyrins with 3 or 4 nonrotating *meso*-aryl groups and all the Fe(III) complexes which cannot be planar because of the presence of at least one axial iron ligand appear unable to intercalate into CT DNA. Their affinity for DNA is lower than those of the intercalating porphyrins but, contrary to them, depends mainly on the number of cationic charges and almost not at all on the position of the *N*-methyl groups in the pyridiniumyl rings. Such behavior is expected for nonintercalating interactions.

Finally, the dramatic differences observed between the two dicationic porphyrins CH_3O2-cis and CH_3O2-trans are compatible with an intercalation for the former and an external binding for the latter. Accordingly, K_{app} of CH_3O2-trans belongs to the correlation line log $K_{app} = f$(charge number) for the CH_3O series, whereas that of CH_3O2-cis is out of this correlation line. Moreover, CH_3O2-cis exhibits a higher affinity as expected for an intercalating species. These results suggest that the presence of two cis nonrotating *meso*-aryl groups on a porphyrin does not prevent its intercalation into CT DNA and that intercalation of half the porphyrin core is possible. This is in agreement with the theoretical model proposed recently by Neidle and co-workers on the basis of molecular modeling and calculations (Ford et al., 1987b). This is also in agreement with our results on porphyrin CH_3P3-OCH_3 which satisfies the four criteria of intercalation (Table II) and which involves only one nonrotating *meso*-aryl group.

Another type of external binding of porphyrins to CT DNA with the formation of long-range stacked structures on the exterior of DNA was recently proposed for porphyrins having a marked tendency to aggregate such as CH_3P2-cis and -trans (Gibbs et al., 1988b). The much larger tendency of CH_3P2 isomers to aggregate than CH_3P4 was shown by clear changes of their UV–visible spectra in buffer upon increasing the ionic strength (with [NaCl] from 0.4 to 1.2 M) (Gibbs et al., 1988b). Formation of such long-range stacked porphyrin structures on the exterior of DNA for CH_3P2-cis or -trans was found particularly significant at high ionic strength and for high [porphyrin]:[DNA base pairs] ratio (r = 0.3–2). The conditions used for most of our spectroscopy measurements (μ = 0.2 and [porphyrin]:[DNA base pairs] = 0.04) do not seem to favor this type of external interaction. Furthermore, a study of the effects of the ionic strength on the UV–visible spectra of the other dicationic porphyrins CH_3M2-cis, CH_3M2-trans, CH_3O2-cis, and CH_3O2-trans alone showed us that the CH_3M2 porphyrins aggregated only at ionic strength much larger than CH_3P2 porphyrins. Moreover, the spectra of CH_3O2-cis and CH_3O2-trans were almost unaffected by an increase of NaCl concentration (up to 1 M) (data not shown). Thus, the very similar effects observed in UV–visible and fluorescence spectroscopy, and in energy-transfer and DNA lengthening experiments in CT DNA–porphyrins interactions for nonaggregating porphyrins such as CH_3P4, CH_3M4, CH_3M2, and CH_3O2-cis and for aggregating porphyrins CH_3P2-cis and CH_3P2-trans, are better explained by an intercalation phenomenon than by an external binding with formation of long-range stacked structures, at least in the conditions used in our study. In particular, the different behavior of CH_3O2-cis and CH_3O2-trans (Table II) which are both poor aggregating porphyrins cannot be explained by considering such an external binding.

In conclusion, the aforementioned results, concerning the interaction between CT DNA and 33 prepared porphyrins or metalloporphyrins involving between two and four *meso*-(*N*-methyl-4(or 3 or 2)-pyridiniumyl) substituents, confirm some conclusions already reported in the literature (see the introduction) about the intercalating ability and high affinity for CT DNA of porphyrins having four freely rotating *meso*-aryl groups such as CH_3P4 and CH_3M4, and about the relatively high affinity of porphyrins that only bind to the exterior of DNA such as CH_3O4. Moreover, our results (i) provide approximate values for the apparent binding constants of all these porphyrins for CT DNA (K_{app} values between 1.2×10^7 and 5×10^4 M^{-1} at μ = 0.2 M), (ii) show that log $K_{app} = f$(number of cationic charges) are straight lines with an almost identical slope, and (iii) demonstrate that all the porphyrins which have at least two cis freely rotating *meso*-aryl groups and no metal ion, or a metal ion without axial ligand, appear able to intercalate into CT DNA, indicating that half of the porphyrin in a completely planar conformation is sufficient for intercalation to occur.

Acknowledgments

We thank Janine Couprie (IGR, Villejuif) for her technical assistance and Alain Gouyette (IGR, Villejuif) and C. Rolando (ENS, Paris) for recording of the mass spectra.

References

Banville, D. L., Marzilli, L. G., & Wilson, W. D. (1983) *Biochem. Biophys. Res. Commun. 113*, 148–154.

Banville, D. L., Marzilli, L. G., Strickland, J. A., & Wilson, W. D. (1986) *Biopolymers 25*, 1837–1858.

Blom, N., Odo, J., Nakamoto, K., & Strommen, D. P. (1986) *J. Phys. Chem. 90*, 2847–2852.

Bromley, S. D., Ward, B. W., & Dabrowiak, J. C. (1986) *Nucleic Acids Res. 14*, 9133–9148.

Butour, J. L., Delain, E., Coulaud, D., Le Pecq, J. B., Barbet, J., & Roques, B. P. (1978) *Biopolymers 17*, 873–886.

Carvlin, M. J., & Fiel, R. J. (1983) *Nucleic Acids Res. 11*, 6121–6139.

Carvlin, M. J., Datta-Gupta, N., & Fiel, R. J. (1982) *Biochem. Biophys. Res. Commun. 108*, 66–73.

Carvlin, M. J., Mark, E., Fiel, R. J., & Howard, J. C. (1983) *Nucleic Acids Res. 11*, 6141–6154.

Dougherty, G., & Pilbrow, J. R. (1985) *Int. J. Biochem. 24*, 1179–1192.

Dougherty, G., Pilbrow, J. R., Skorobogaty, A., & Smith, T. D. (1985) *J. Chem. Soc., Faraday Trans. 2 81*, 1739–1759.

Fiel, R. J. (1989) *J. Biomol. Struct. Dyn. 6*, 1259–1274.

Fiel, R. J., & Munson, B. R. (1980) *Nucleic Acids Res. 8*, 2835–2842.

Fiel, R. J., Howard, J. C., Mark, E. H., & Datta-Gupta, N. (1979) *Nucleic Acids Res. 6*, 3093–3118.

Fiel, R. J., Carvlin, M. J., Byrnes, R. W., & Mark, E. H. (1985) in *Molecular Basis of Center, Part B, Macromolecular Recognition, Chemotherapy and Immunology*, pp 215–226, Alan R. Liss, New York.

Ford, K., Fox, K. R., Neidle, S., & Waring, M. J. (1987a) *Nucleic Acids Res. 15*, 2221–2234.

Ford, K. G., Pearl, L. H., & Neidle, S. (1987b) *Nucleic Acids Res. 15*, 6553–6562.

Geacintov, N. E., Ibanez, V., Rougée, M., & Bensasson, R. V. (1987) *Biochemistry 26*, 3087–3092.

Gibbs, E., Fasella, P., Cerio Venturo, G., & Dev C. Hinds, L. (1972) *J. Am. Chem. Soc. 94*, 4511–4517.

Gibbs, E. J., Maurer, M. C., Zhang, J. H., Reiff, W. M., Hill, D. T., Malicka-Blaszkiewicz, M., McKinnie, R. E., Liu, H.-Q., & Pasternack, R. F. (1988a) *J. Inorg. Biochem. 32*, 39–65.

Gibbs, E. J., Tinoco, I., Jr., Maestre, M. F., Ellinas, P. A., & Pasternack, R. F. (1988b) *Biochem. Biophys. Res. Commun. 157*, 350–358.

Hambright, P. H., & Fleischer, E. B. (1970) *Inorg. Chem. 9*, 1757-1761.
Hambright, P. H., Gore, T., & Burton, M. (1976) *Inorg. Chem. 15*, 2314-2315.
Kalyanasundaram, K. (1984) *Inorg. Chem. 23*, 2453-2459.
Kelly, J. M., Murphy, M. J., McConnell, D. J., & OhUigin, C. (1985) *Nucleic Acids Res. 13*, 167-184.
Le Pecq, J. B., & Paoletti, C. (1967) *J. Mol. Biol. 27*, 87-106.
Little, R. G., Anton, J. A., Loach, P. A., & Ibers, J. A. (1975) *J. Heterocycl. Chem. 12*, 343-349.
Marzilli, L. G., Banville, D. L., Zon, G., & Wilson, W. D. (1986) *J. Am. Chem. Soc. 108*, 4188-4192.
Pasternack, R. F., Huber, P. R., Boyd, P., Engasser, L., Francesconi, L., Gibbs, E., Fasella, P., Cerio Venturo, G., & Hinds, L. deC. (1972) *J. Am. Chem. Soc. 94*, 4511-4517.
Pasternack, R. F., Cobb, M. A., & Sutin, N. (1975) *Inorg. Chem. 14*, 866-873.
Pasternack, R. F., Lee, H., Malek, P., & Spencer, C. (1977) *J. Inorg. Nucl. Chem. 39*, 1865-1870.
Pasternack, R. F., Gibbs, E. J., & Villafranca, J. J. (1983a) *Biochemistry 22*, 2406-2414.
Pasternack, R. F., Gibbs, E. J., & Villafranca, J. J. (1983b) *Biochemistry 22*, 5409-5417.
Pasternack, R. F., Antebi, A., Ehrlich, B., Sidney, D., Gibbs, E. J. Bassner, S. L., & DePoy, L. M. (1984) *J. Mol. Catal. 23*, 235-242.
Pasternack, R. F., Gibbs, E. J., Gaudemer, A., Antebi, A., Bassner, S., DePoy, L., Turner, D. H., Willilams, A., Laplace, F., Lansard, M. H., Merienne, C., & Perrée-Fauvet, M. (1985) *J. Am. Chem. Soc. 107*, 8179-8186.
Pasternack, R. F., Garrity, P., Ehrlich, B., Davis, C. B., Gibbs, E. J., Orloff, G., Giartosio, A., & Turano, C. (1986) *Nucleic Acids Res. 14*, 5919-5931.
Reinhardt, C. G., Roques, B. P., & Le Pecq, J. B. (1982) *Biochem. Biophys. Res. Commun. 104*, 1376-1385.
Sari, M. A., Battioni, J. P., Mansuy, D., & Le Pecq, J. B. (1986) *Biochem. Biophys. Res. Commun. 141*, 643-649.
Sari, M. A., Battioni, J. P., Dupré, D., Mansuy, D., & Le Pecq, J. B. (1988) *Biochem. Pharmacol. 37*, 1861-1862.
Saucier, J. M., Festy, B., & Le Pecq, J. B. (1971) *Biochimie 53*, 973-980.
Shamim, A., Hambright, P., & Williams, F. X. (1979) *Inorg. Nucl. Chem. Lett. 15*, 243-246.
Shamim, A., Worthington, P., & Hambright, P. (1981) *J. Chem. Soc. Pak. 3*, 1-3.
Strickland, J. A., Banville, D. L., Wilson, W. D., & Marzilli, L. G. (1987) *Inorg. Chem. 26*, 3398-3406.
Strickland, J. A., Marzilli, L. G., Gay, K. M., & Wilson, W. D. (1988) *Biochemistry 27*, 8870-8878.
Strickland, J. A., Marzilli, L. G., & Wilson, W. D. (1989) *Biopolymers* (in press).
Verlhac, J. P. (1984) Thèse de 3ème cycle, Orsay, France.
Ward, B., Skorobogaty, A., & Dabrowiak, J. C. (1986) *Biochemistry 25*, 7827-7833.

Solution Conformation of an RNA Hairpin Loop†

Joseph D. Puglisi,‡ Jacqueline R. Wyatt, and Ignacio Tinoco, Jr.*
Department of Chemistry and Laboratory of Chemical Biodynamics, University of California, Berkeley, California 94720
Received October 17, 1989; Revised Manuscript Received January 2, 1990

ABSTRACT: The hairpin conformation adopted by the RNA sequence $^{5'}$**GCGAUUUCUGACCGCC**$^{3'}$ has been studied by one- and two-dimensional NMR spectroscopy. Exchangeable imino spectra in 60 mM Na^+ indicate that the hairpin has a stem of six base pairs (indicated by boldface type) and a loop of three nucleotides. NOESY spectra of nonexchangeable protons confirm the formation of the stem region. The duplex has an A-conformation and contains an A·C apposition; a G·U base pair closes the loop region. The stem nucleotides have C3′-endo sugar conformations, as expected of an A-form duplex, whereas the three loop nucleotides adopt C2′-endo sugar puckers. Stacking within the loop, C_8 upon the sugar of U_7, stabilizes the structure. The pH dependence of both the exchangeable and nonexchangeable NMR spectra is consistent with the formation of an A^+·C base pair, protonated at the N1 position of adenine. The stability of the hairpin was probed by using absorbance melting curves. The hairpin structure with the A^+·C base pair is about +2 kcal/mol less stable in free energy at 37 °C than the hairpin formed with an A·U pair replacing the A^+·C pair.

Hairpins are common elements of RNA secondary structure. These stem–loop structures are often the building blocks for the three-dimensional folded architecture of RNA. The well-characterized secondary structure of the 16S rRNA from *Escherichia coli* (1542 nucleotides) contains 31 hairpin loop structures (Noller, 1984). The much simpler cloverleaf secondary structure of tRNA contains three hairpin loops. The crystal structures of tRNAs show that hairpin loops are not inert structural elements but can be actively involved in the tertiary structure; the interactions between the D and T loop regions are important to the three-dimensional L-shaped folding of $tRNA^{Phe}$. It has become increasingly clear that stem–loop structures are important sites for specific RNA–protein interactions. The bacteriophage R17 coat protein represses translation of the R17 replicase gene by specific binding to a hairpin that contains the initiation codon (Romaniuk et al., 1987). Both sequence and stem–loop structure determine specific binding interactions (Wu & Uhlenbeck,

† This work was supported in part by the National Institutes of Health under Grant GM 10840 and by the Department of Energy, Office of Energy Research, Office of Health and Environmental Research, under Grant DE-FG03-86ER60406.
* To whom correspondence should be addressed at the Department of Chemistry.
‡ Present address: Institut de Biologie Moleculaire et Cellulaire du CNRS, 15, rue René Descartes, 67084 Strasbourg, France.

0006-2960/90/0429-4215$02.50/0